Ocean Engineering 141 (2017) 465–476

Contents lists available at ScienceDirect

Ocean Engineering

journal homepage: www.elsevier.com/locate/oceaneng

# Estimation of added resistance and ship speed loss in a seaway

Mingyu Kim[a,*], Olgun Hizir[b], Osman Turan[a], Sandy Day[a], Atilla Incecik[a]

[a] Department of Naval Architecture, Ocean and Marine Engineering, University of Strathclyde, 100 Montrose Street, Glasgow G4 0LZ, UK
[b] Ponente Consulting Ltd., Ipswich, Suffolk IP2 0EL, UK

ARTICLE INFO

*Keywords:*
Added resistance
Ship motions
Ship speed loss
Potential flow
CFD

ABSTRACT

The prediction of the added resistance and attainable ship speed under actual weather conditions is essential to evaluate the true ship performance in operating conditions and assess environmental impact. In this study, a reliable methodology is proposed to estimate the ship speed loss of the S175 container ship in specific sea conditions of wind and waves. Firstly, the numerical simulations are performed to predict the added resistance and ship motions in regular head and oblique seas using three different methods; a 2-D and 3-D potential flow method and a Computational Fluid Dynamics (CFD) with an Unsteady Reynolds-Averaged Navier-Stokes (URANS) approach. Simulations of various wave conditions are compared with the available experimental data and these are used in a validation study. Secondly, following the validation study in regular waves, the ship speed loss is estimated using the developed methodology by calculating the resistance in calm water and the added resistance due to wind and irregular waves, taking into account relevant wave parameters and wind speed corresponding to the Beaufort scale, and results are compared with simulation results obtained by other researchers. Finally, the effect of the variation in ship speed and therefore the ship speed loss is investigated. This study shows the capabilities of the 2-D and 3-D potential methods and CFD to calculate the added resistance and ship motions in regular waves in various wave headings. It also demonstrates that the proposed methodology can estimate the impacts on the ship operating speed and the required sea margin in irregular seas.

## 1. Introduction

Now more than ever, the reduction of ship pollution and emissions, maximization of energy efficiency, enhancement of safety requirements and minimization of operational expenditure are key priorities. Traditionally, the focus has been on ship resistance and propulsion performance in calm water during the ship design stage even though there have recently been some changes in hull form design and optimization, from a single design draught and speed to a specific range of draughts and speeds considering a realistic operating profile for the vessel. However, when a ship advances through a seaway, she requires additional power in comparison with the power required in calm water due to actual weather and ship operating conditions. This degradation of the ship performance in a seaway, which is reported to be an addition of about 15–30% of the power required in calm water (Arribas, 2007) is accounted for by the application of a “Sea Margin” onto the total required engine power and a value of 15% is typically used. A more accurate prediction of the added resistance with motions and ship speed loss is essential not only to assess the true sea margin to determine the engine and propeller design points, but also to evaluate the ship performance and environmental impact under actual weather and operating conditions. Also from a ship designer's point of view, the design could be seen as more competitive if the vessel is designed for better performance in a seaway, and for ship owners and officers, they could have safer ships in actual operation at sea.

Regarding the international regulations, the Marine Environment Protection Committee (MEPC) of the International Maritime Organization (IMO) issued new regulations to improve the energy efficiency level of ships and to reduce carbon emissions. These regulations include the Energy Efficiency Design Index (EEDI) (IMO, 2011) as a mandatory technical measure for new ships and the Energy Efficiency Operational Indicator (EEOI) (IMO, 2009) which is related to ship voyage and operational efficiency for ships in service. Recently, the ship speed reduction coefficient ($f_w$) has been proposed and is under discussion for the calculation of EEDI in representative sea states (IMO, 2012; ITTC, 2014).

The added resistance and ship motion problem in waves has been widely studied through experiments and numerical simulations using potential flow theory and CFD approaches. There are two major analytical approaches in potential flow methods which are used to

* Corresponding author.
*E-mail address:* mingyu.kim@strath.ac.uk (M. Kim).

http://dx.doi.org/10.1016/j.oceaneng.2017.06.051
Received 9 December 2016; Received in revised form 23 May 2017; Accepted 19 June 2017
Available online 27 June 2017

calculate the added resistance: the far-field method and the near-field method. The far-field method is based on the added resistance computed from the wave energy and the momentum flux generated from a ship, and is evaluated across a vertical control surface of infinite radius surrounding the ship. The first study was introduced by Mauro (1960) using a Kochin function which consists of radiating and diffracting wave components and investigated in detail by Joosen (1966) and Newman (1967). Later on, the far-field method, based on radiated energy approach was proposed by Gerritsma and Beukelman (1972) for added resistance in head seas and has become popular in strip theory programs due to its easy implementation. This approach was modified and extended to oblique waves by Loukakis and Sclavounos (1978). Recently, Kashiwagi et al. (2010) used the far-field method to calculate the added resistance using enhanced unified theory to overcome the discrepancies originating in short waves and in the presence of forward speed with the experiments by introducing a correction factor in the diffracted wave component. They observed that the discrepancies tended to increase and became constant with the increase in the forward speed. The disadvantage of the far-field method is the dependency of the added resistance on the wave damping which cause inaccurate radiation forces at low frequencies when using the strip theory method. Liu et al. (2011) solved the added resistance problem using a quasi-second-order approach, applying the developed hybrid Rankine Source-Green function method considering the asymptotic and empirical methods to improve the results in short waves.

Another numerical approach is the near-field method which estimates the added resistance by integrating the hydrodynamic pressure on the body surface, which was first introduced by Havelock (1937) where the Froude-Krylov approach was used to calculate hull pressures. Boese (1970) proposed a simplified method where the importance of relative wave height contribution to the added resistance was first addressed. The near-field method was enhanced by Faltinsen et al. (1980) based on the direct pressure integration approach. Salvesen et al. (1970) introduced a simplified asymptotic method based on 2-D strip theory to overcome the deficiency of this approach in short waves. Kim et al. (2007) and Joncquez (2009) formulated the added resistance based on the Rankine panel method using a time-domain approach with B-spline functions and investigated the effects of the Neumann-Kelvin (NK) and Double Body (DB) linearization schemes on the added resistance predictions. Recently, Kim et al. (2012) formulated the added resistance using a time-domain B-spline Rankine panel method based on both near-field and far-field methods in addition to the NK and DB linearization schemes for the forward speed problem. They observed that, in the case of the added resistance, the far-field method was superior to the near-field method in short waves whilst, in the case of the free-surface linearization scheme, NK linearization showed better agreement with the experiments at high speeds compared to the DB linearization for slender bodies.

As computational facilities have become more powerful and more accessible, CFD techniques have been more commonly used to predict the added resistance and ship motions, taking into account viscous effects without empirical values and large ship motions as well as the effect of breaking waves and green water effect. Recently, Deng et al. (2010), Moctar et al. (2010) and Sadat-Hosseini et al. (2010) predicted the added resistance of KVLCC2 CFD tools as presented at the Gothenburgh (2010), SIMMAN (2014) and SHOPERA (2016) Workshops. Following that, Guo et al. (2012) predicted motions and the added resistance for KVLCC2 using the ISIS-CFD flow solver as a RANS code and Sadat-Hosseini et al. (2013) predicted the added resistance and motions for KVLCC2 using the in-house code CFDSHIP-IOWA which is based on a URANS approach. Simonsen et al. (2013) carried out numerical simulations for the ship motions, flow field and added resistance for the KCS containership using Experimental Fluid Dynamics (EFD) and CFD. Tezdogan et al. (2015) performed URANS simulations to estimate the effective power and fuel consumption of the full scale KCS containership in waves by predicting added resistance in regular head seas using the commercial STAR-CCM+ software.

In addition to research on accurate prediction of the added resistance and ship motions in waves, there have been studies on reduction of the added resistance by developing the hull form. Park et al. (2014) modified the forebody of the KVLCC2 to an Axe-bow and Leadge-bow to reduce the added resistance in waves by means of EFD and potential theories. Kim et al. (2014) revised the bulbous bow of a containership to optimize the hull form for both operating profile of the ship in calm water and wave conditions using CFD simulations. However, there has been no significant research on the increase of the required power and the ship speed loss in a seaway.

In the present study, in line with the energy efficiency regulations, the main focus is on the development of a reliable methodology to estimate the added resistance and the ship speed loss due to wind and waves. All calculations have been performed for the S175 containership. Firstly, numerical calculations and validation studies have been carried out for the added resistance with ship motions in regular head and oblique waves using 2-D and 3-D linearized potential flow methods and CFD. Secondly, after the validation study on the added resistance in regular waves, the ship speed loss is estimated by the proposed methodology predicting the resistance in calm water and the added resistance due to wind and irregular waves taking into account the wave height, mean wave period and wind speed corresponding to the Beaufort scale, based on IMO and ITTC guideline/recommendation (IMO, 2012; ITTC, 2014) and compared with simulation results obtained by Kwon (2008) and Prpić-Oršić and Faltinsen (2012). Finally, taking into consideration the typical slow steaming speeds of containerships, studied in detail by Banks et al. (2013) who compared the operating speeds from 2006–2008 to 2009–2012, the effect of the ship speed loss at preliminary design and other lower speeds was investigated.

## 2. Ship particulars and coordinate system

All calculations of the added resistance and ship speed loss have been performed for the S175 containership, which is one of the benchmark hull forms used to study seakeeping capability by several researchers. The main particulars of the S175 containership are given in Table 1. The model with scale ratio of 1/40 is employed in CFD simulations to estimate the added resistance and ship motions in regular waves and in head and wave headings.

In the numerical simulations, a right-handed coordinate system x, y, z is adopted, as shown in Fig. 1, where the translational displacements in the x, y and z directions are $\xi_1$ (surge), $\xi_2$ (sway) and $\xi_3$ (heave), and the angular displacements of rotational motion about the x, y and z axes are $\xi_4$ (roll), $\xi_5$ (pitch) and $\xi_6$ (yaw) respectively and the angle $\theta$ represents the ship's heading angle with respect to the incident waves. For head seas the angle $\theta$ equals 0° and for beam seas from the port side the angle equals 90°.

**Table 1**
Main particulars of S175 containership.

| Particulars | Full scale | Model scale |
|---|---|---|
| Length, $L$ (m) | 175 | 4.375 |
| Breadth, $B$ (m) | 25.4 | 0.635 |
| Draught, $T$ (m) | 9.5 | 0.2375 |
| Displacement, $V$ ($m^3$) | 23,680 | 0.3774 |
| $LCG$(%), fwd + | −1.337 | −1.337 |
| $VCG$ (m) | 9.52 | 0.238 |
| Block coefficient, $C_B$ (-) | 0.572 | 0.572 |

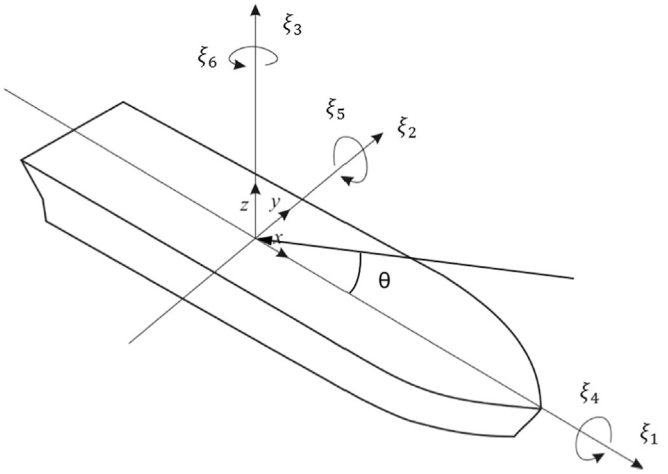


**Fig. 1.** Vessel coordinate system.

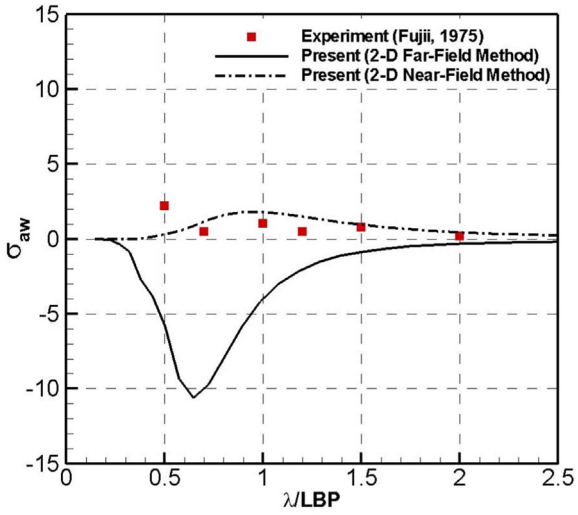


**Fig. 2.** Added resistance comparison for S175 (Fn = 0.25, θ = 180°) using 2D linear potential method and experiments.

## 3. Numerical methods and modelling

In the present study, three different methods, namely the 2-D and 3-D linear potential methods and the CFD method were applied for the validation study on the added resistance and ship motions in regular waves and in various wave headings. For the numerical calculation of the added resistance due to irregular waves, the 2-D linear potential method was used and the mean added resistance due to irregular waves was evaluated by numerical integration. In the current study, wind spectrums were not applied in the estimation of total wind forces for the sake of simplicity.

### 3.1. 2D linear potential method

The calculation of the added resistance and ship motions in waves was carried out using the 2-D linear potential method software ShipX. The program was developed by MARINTEK (Norwegian Marine Technology Research Institute) as a common platform for ship design analysis on ship motions and global loads in early design stage based on the 2-D linear potential using the strip theory (Salvesen et al., 1970). In the ShipX program, the calculation of the added resistance in waves can be performed using two different approaches. The first approach is the far-field method based on the momentum conservation theory developed by Gerritsma and Beukelman (1972) and generalized and extended to oblique waves by Loukakis and Sclavounos (1978). The second approach is the near-field method to integrate hydrodynamic pressure on the body surface including asymptotic formula in short waves to overcome the deficiency of the approach as discussed previously (Faltinsen et al., 1980). In the current study, the second approach is chosen for the calculation of the added resistance because the first approach shows large difference in the peak values while negative values conflict with the experimental data for the case of the following waves as shown in Fig. 2.

The main reason for the poor agreement in the prediction of the added resistance for following seas between the far-field method and experimental results is attributed to the inaccuracies in the hydrodynamic coefficients and motions in the strip theory method which assumes low Froude number, high frequency and slender body (McTaggart et al., 1997). In following seas the encounter frequency is low and in the current study the ship speed is high, hence the Pulsating Source (PS) method in the strip theory fails to satisfy the forward speed Free Surface Boundary Condition (FSBC). In the far-field method the added resistance prediction depends on the wave induced damping terms, hence when the encounter frequency is low, radiation forces cannot be calculated accurately and this results in negative added resistance values. However, the near-field method uses the drift forces obtained by the direct pressure integration method on the hull surface where drift forces are dominated by the ship relative motion. The strip theory predicts relative motions superior to the damping coefficients therefore the near-field method agreed better with the experiments compared to the far-field method. The mean added resistance ($\Delta R_{wave}$) was non-dimensionalised as follows;

$$\sigma_{aw} = \frac{\Delta R_{wave}}{\rho g A^2 B^2 / L} \tag{1}$$

where ρ, g and A denote the density, gravitational acceleration, and the wave amplitude parameters respectively.

In the present study, the mean added resistance of the vessel due to waves will be represented by the added resistance coefficient ($\sigma_{aw}$) for the comparison with other researchers results.

### 3.2. 3D linear potential method

3-D potential flow calculations are carried out using the PRECAL (PREssure CALculation) software developed by the Maritime Research Institute Netherlands (MARIN) (Van't Veer, 2009). The PRECAL software is based on the planar panel approach which can calculate the seakeeping behaviour of monohull, catamaran and trimaran ships. PRECAL is a 3-D source-sink frequency domain code capable of solving the forward speed linear Boundary Value Problem (BVP) using the Approximate Forward Speed (AFS) and the Exact Forward Speed (EFS) methods. In the AFS method the BVP is solved using zero-speed Green's functions and then forward speed corrections are applied to the BVP equations. It is possible to use the Lid panel method (Lee and Sclavounos, 1989) where waterplane area (Lid) panels are used to suppress the occurrence of the irregular frequencies in the BVP solutions. In the EFS method, exact forward speed Green's functions are used to solve the forward speed BVP, but in the PRECAL software the Lid panel method can only be applied to the AFS formulation. In this study, forward speed ship motions are solved using the AFS formulation due to its fast and accurate results (Hizir, 2015). The added resistance is calculated using the near-field method based on direct pressure integration over the mean wetted hull surface, using the second-order forces to calculate wave drift forces while the first-order forces and moments are calculated to solve the ship motions.

In added resistance calculations, only the mean values of the forces and moments are of interest. First-order quantities such as motions, velocities, accelerations, etc. have a mean value of zero when the wave is given by an oscillatory function with a mean value of zero. However, second-order quantities such as added resistance have a non-zero mean

value therefore in order to calculate the added resistance, second-order forces and moments need to be calculated. In the present study, in the calculation of added resistance only the constant part (mean value) of the added resistance is taken into account while the slowly oscillating part of the added resistance is trivial.

### 3.3. Computational Fluid Dynamics (CFD)

An URANS approach was applied to calculate the added resistance and ship motions in regular waves using the commercial CFD software STAR-CCM+. For incompressible flows, if there are no external forces, the averaged continuity and momentum equations are given in tensor form in the Cartesian coordinate system by Eq. (2) and Eq. (3)

$$\frac{\partial(\rho\overline{u}_i)}{\partial x_i} = 0 \tag{2}$$

$$\frac{\partial(\rho\overline{u}_i)}{\partial t} + \frac{\partial}{\partial x_j}(\rho\overline{u}_i\overline{u}_j + \rho\overline{u_i'u_j'}) = -\frac{\partial\overline{p}}{\partial x_i} + \frac{\partial\overline{\tau}_{ij}}{\partial x_j} \tag{3}$$

where $\overline{u}_i$ is the averaged velocity vector of fluid, $\overline{u_i'u_j'}$ is the Reynolds stresses and $\overline{p}$ is the mean pressure.

The finite volume method (FVM) and the volume of fluid (VOF) method were applied for the spatial discretization and free surface capturing respectively. The flow equations were solved in a segregated manner using a predictor-corrector approach. Convection and diffusion terms in the RANS equations were discretised by a second-order upwind scheme and a central difference scheme. The semi-implicit method for pressure-linked equations (SIMPLE) algorithm was used to resolve the pressure-velocity coupling and a standard $k-\varepsilon$ model was applied as the turbulence model. In order to consider ship motions, a Dynamic Fluid Body Interaction (DFBI) scheme was applied with the vessel free to move in heave and pitch directions as vertical motions.

Only half of the ship's hull (the starboard side) with a scale ratio of 1/40 and a corresponding control volume were taken into account in the calculations, thus a symmetry plane formed the centreline domain face in order to reduce computational time and complexity. The calculation domain is $-2L_{PP} < x < 1.0L_{PP}$, $0 < y < 1.5L_{PP}$, $-1.5L_{PP} < z < 1.0L_{PP}$ where the mid-plane of the ship is located at $y = 0$ and ship draught (T) is at z =0. The boundary conditions together with the generated meshes are depicted in Fig. 3. Artificial wave damping was applied to avoid the undesirable effect of the reflected waves from the side and outlet boundaries.

The added resistance due to waves ($\Delta R_{wave}$) is obtained by Eq. (4)

$$\Delta R_{wave} = R_{wave} - R_c \tag{4}$$

where $R_{wave}$ and $R_c$ are resistance in wave conditions and calm water respectively, which are all predicted using CFD.

The CFD simulations including calm water condition were performed as summarized in Table 2 where each identified by their case numbers. The ratio of non-dimensionalised wave length ($\lambda/L_{PP}$) is selected to be between 0.5 and 1.5, and the wave steepness in all cases was chosen to be 1/60. In all cases, the ship speed is 1.6375 m/s with Fn = 0.25 which corresponds to a ship speed of 20.14 knots. Regarding wave direction, the cases of following waves are considered for the validation of the CFD simulations and the comparison with the results of the 2-D and 3-D potential methods, and the experimental data.

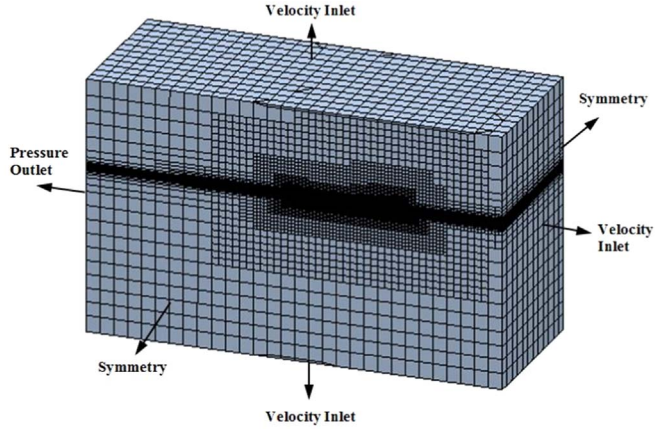


**Fig. 3.** Mesh and boundary conditions.

**Table 2**
CFD test conditions in calm water and regular waves (Fn = 0.25, H/λ = 1/60).

| Case no. (C) | Wave length ($\lambda/L_{pp}$) | Wave height [m] | Wave direction |
|---|---|---|---|
| 0 | Calm water | No waves | – |
| 1 | 0.50 | 0.03646 | Head/following wave |
| 2 | 0.70 | 0.05104 | Head wave |
| 3 | 0.85 | 0.06198 | Head/following wave |
| 4 | 1.00 | 0.07292 | Head wave |
| 5 | 1.15 | 0.08385 | Head/following wave |
| 6 | 1.30 | 0.09479 | Head wave |
| 7 | 1.50 | 0.10938 | Head wave |

**Table 3**
Test cases for grid convergence (λ/L = 0.5 and 1.2).

| Case no. | Mesh | λ/Δx | H/Δz | Te/Δt |
|---|---|---|---|---|
| Case 2 & 5 | Coarse(C) | 70 | 14 | 181 |
| Case 2 & 5 | Base | 100 | 20 | 256 ($2^8$) |
| Case 2 & 5 | Fine(F) | 140 | 28 | 362 |

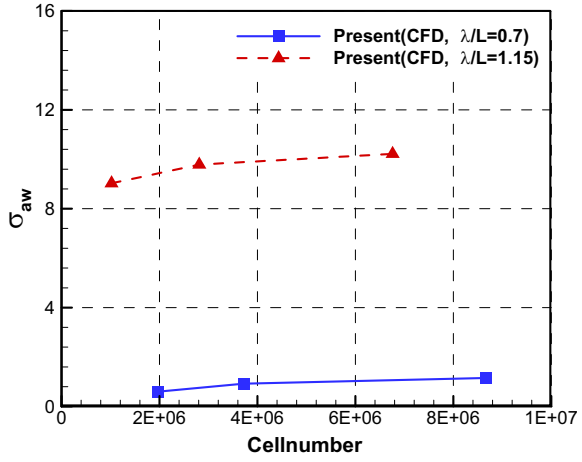


**Fig. 4.** Grid convergence test for the added resistance in short (λ/L = 0.5) and long (λ/L = 1.2) waves.

Prior to the investigation of the added resistance with the heave and pitch motions using the CFD method, grid convergence tests were performed to capture the accurate wave length and height on the free surface for not only long wave (λ/L = 1.15), but also for short (λ/L = 0.7) wave conditions because in short waves when coarse mesh is used the added resistance might be underestimated. The coarse and fine mesh systems are derived by reducing and increasing cell numbers per wave length and cell height on free surface respectively using a factor of $\sqrt{2}$ based on the base mesh. The simulation time step is set to be proportional to the grid size as shown in Table 3 where Te represents the corresponding encountering period.

The results of the convergence tests with three different mesh systems in short and long waves are shown in Fig. 4. As the number of cells increased, the added resistance coefficient increased, especially from the coarse mesh to base mesh system for short wave case. The test results of the added resistance for the base and fine mesh show a monotonic convergence with the convergence ratio ($R_G$) of 0.690 and

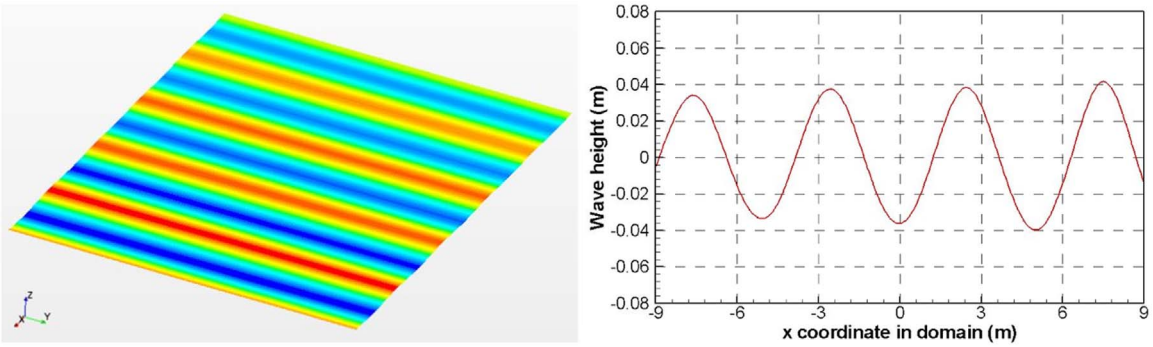


**Fig. 5.** Wave calibration results (wave conditions for the Case 5).

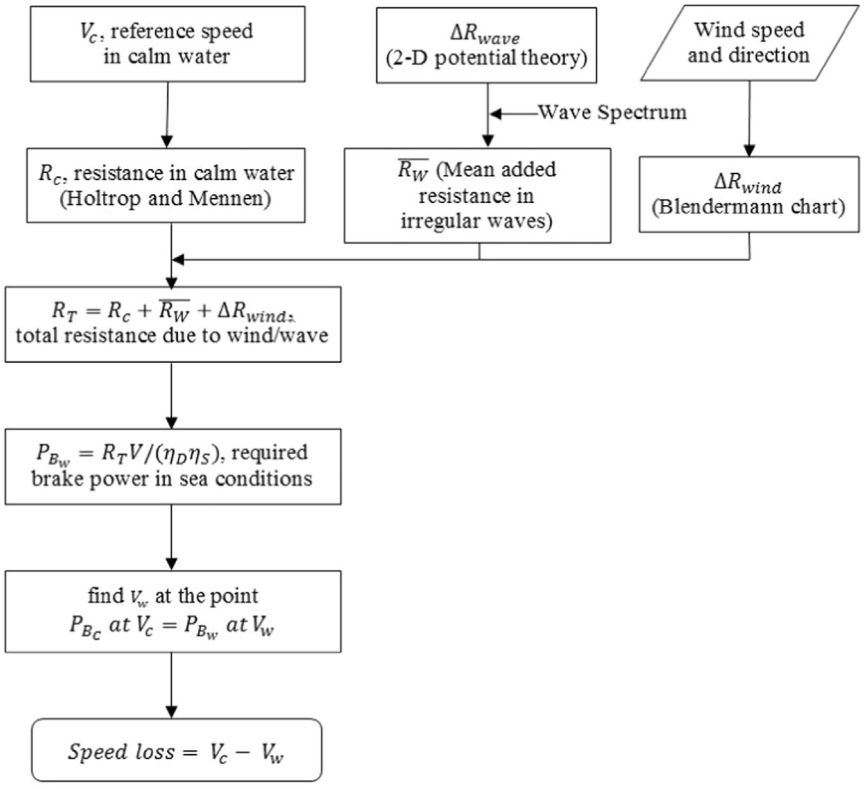


**Fig. 6.** Ship speed loss estimation flowchart.

**Table 4**
Typical sea conditions corresponding Beaufort number.

| Beaufort number, B.N. | Mean wind speed, $U_{wind}$ [m/s] | Significant wave height, Hs [m] | Mean wave period, Tm [s] |
|---|---|---|---|
| 0 | 0.0 | 0.0 | 0.000 |
| 1 | 0.9 | 0.1 | 1.22 |
| 2 | 2.3 | 0.4 | 2.44 |
| 3 | 4.4 | 0.8 | 3.45 |
| 4 | 6.7 | 1.5 | 4.73 |
| 5 | 9.4 | 2.0 | 5.46 |
| 6 | 12.6 | 3.0 | 6.67 |
| 7 | 15.5 | 4.5 | 8.19 |

0.577 in short and long waves respectively (Stern et al., 2006), which indicates that the effects of the grid change are accepted to be small between base and fine mesh system (Tezdogan et al., 2015). Therefore the base mesh system was chosen for the CFD simulations in this study for both short and long wave cases and the cell number and time step vary according to the wave conditions in the simulations.

Also before calculating the added resistance of the ship due to waves, a wave calibration test was performed for the wave conditions of case 5 (C5) in Table 2. Fig. 5 shows the wave contour of the free surface and the results of wave elevation in calculation domain. The difference of the simulated wave height between the inlet and ship and the input wave of the case 5 is 2–3.5%, which means the cell size and time step used are acceptable for the current CFD simulation model (Tezdogan et al., 2015).

## 4. Estimation of ship speed loss

The flowchart in Fig. 6 illustrates the procedure of the developed methodology to estimate the ship speed loss due to wind and irregular waves considering the specific sea condition. $\Delta R_{wave}$ and $\Delta R_{wind}$ are the added resistance due to wave and wind, and $\eta_D$ and $\eta_S$ are the propulsion and transmission efficiency. The resistance in calm water $R_c$ and propulsion efficiency $\eta_D$ are estimated based on Holtrop and Mennen's method (Holtrop, 1984; Holtrop and Mennen, 1978, 1982) and transmission efficiency $\eta_S$ of the ship is assumed to be 0.99.

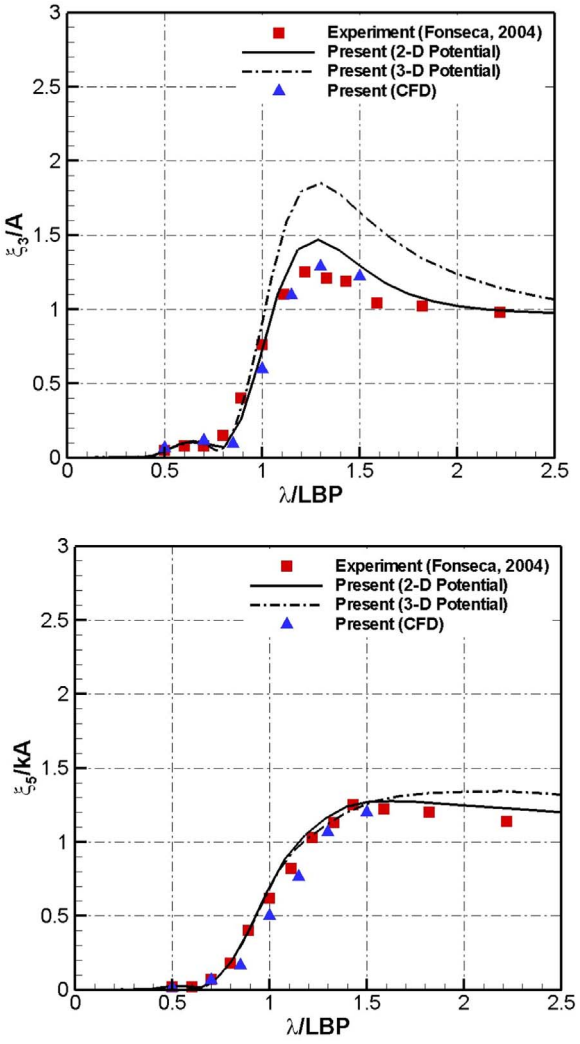


**Fig. 7.** Heave and pitch responses (Fn = 0.25, θ = 0°).

### 4.1. Prediction of the resistance in calm water

In order to calculate the ship speed reduction as additional power required due to wind and wave, the resistance and required power in calm water have to be estimated in advance. In this developed methodology, the resistance and required power are estimated based on Holtrop and Mennen's method (Holtrop, 1984; Holtrop and Mennen, 1978, 1982) which is a regression approach based on model experiments and full-scale data, and which is a useful method for estimating resistance and propulsive power at the initial design stage.

### 4.2. Added resistance due to waves and wind

Regarding the numerical calculation of the added resistance due to irregular waves, the 2-D linear potential method was used. Although some of the assumptions and simplifications are applied, the linear potential theory agreed well with the experimental data with lower computational cost compared to the CFD method.

Since the speed reduction coefficient (fw) was introduced by IMO (2011) and adopted for the calculation of EEDI, the application procedures for the calculation of fw have been discussed in representative sea conditions defined by a wave height, mean wave period and wind speed for head wind and waves. As the representative sea condition, Beaufort Number (B.N.) 6 was adopted by IMO (2012) considering the mean sea conditions of the North Atlantic and North Pacific. In this study, the two parameter Pierson-Moskowitz spectrum based on significant wave height (Hs) and mean wave period (Tm) in short-crested waves with cosine-squared function is used under the assumption that the sea condition of interest is a fully developed sea. Table 4 shows typical sea conditions corresponding to Beaufort number up to 7 including the representative parameters at B.N. 6 for the consideration of fw in EEDI formula.

The relation between B.N. and significant wave height is taken from data published by Wright et al. (1999) which described sea state, significant wave height and wind speed corresponding to each B.N. in fully developed sea. Additionally, the relationship between Hs and Tm is taken from the formula which is recommended by the ITTC (2014) as expressed by Eq. (5).

$$T_m = 3.86\sqrt{H_S} \tag{5}$$

The mean added resistance in irregular waves ($\overline{R_W}$) is evaluated by numerical integration of the Pierson-Moskowitz spectrum and the mean added resistance forces in regular waves ($\Delta R_{wave}$). The mean added resistance force for a particular wave heading, Hs and Tm is given by Eq. (6).

$$\overline{R_W} = 2\int_0^\infty \Delta R_{wave}(\theta, \omega) S(\omega) d\omega \tag{6}$$

where S(ω) is the Pierson-Moskowitz spectral density based on the provided values for $H_s$ and $T_m$.

The added resistance ($\Delta R_{wind}$) due to wind is calculated by Eq. (7) (IMO, 2012):

$$\Delta R_{wind} = \frac{1}{2}\rho_a A_T C_{D_{wind}} \{(U_{wind} + V_w)^2 - V^2_c\} \tag{7}$$

where $\rho_a$ is the density of air, $A_T$ is the frontal projected area of the ship, which is assumed to be 700 $m^2$ based on other similarly sized container ships, $C_{D_{wind}}$ is wind drag coefficient from the chart by Blendermann (1994), which were determined by the regression of wind tunnel test data for a variety of ship types and sizes, and $U_{wind}$ is wind speed.

### 4.3. Estimation for ship speed loss

From the predicted calm water resistance ($R_c$) and the estimated results of the added resistance ($\Delta R_{wind}$ and $\Delta R_{wave}$), the total resistance ($R_T$) due to wind and waves can be estimated as Eq. (8).

$$R_T = R_c + \Delta R_{wind} + \overline{R_W} \tag{8}$$

The ship speed loss for each B.N. is estimated based on the assumption that the required power at the reference ship speed in calm water is the same as the required power in the specific sea condition as given by Eq. (9) after summation of calm water resistance and added resistance due to wind and waves.

$$P_{B_C} at V_c = P_{B_W} at V_w \tag{9}$$

where $P_{B_C}$ and $P_{B_W}$ are the required brake power in calm water and the specific sea conditions, and $V_c$ and $V_w$ are the reference ship speed in calm water and achievable ship speed in the specific sea conditions at the same required brake power as in calm water. Therefore, the ship speed loss can be estimated as Eq. (10).

$$Speed loss = V_c - V_w \tag{10}$$

## 5. Discussion of results

In this section, the results of the motion responses, added resistance and ship speed loss estimations are presented and compared with the available experimental data in regular head waves. The added resistance under ship motions is predicted in regular waves and the ship speed loss is estimated at the assumed design and other lower speeds by the proposed methodology. They will be discussed separately in the following sections.

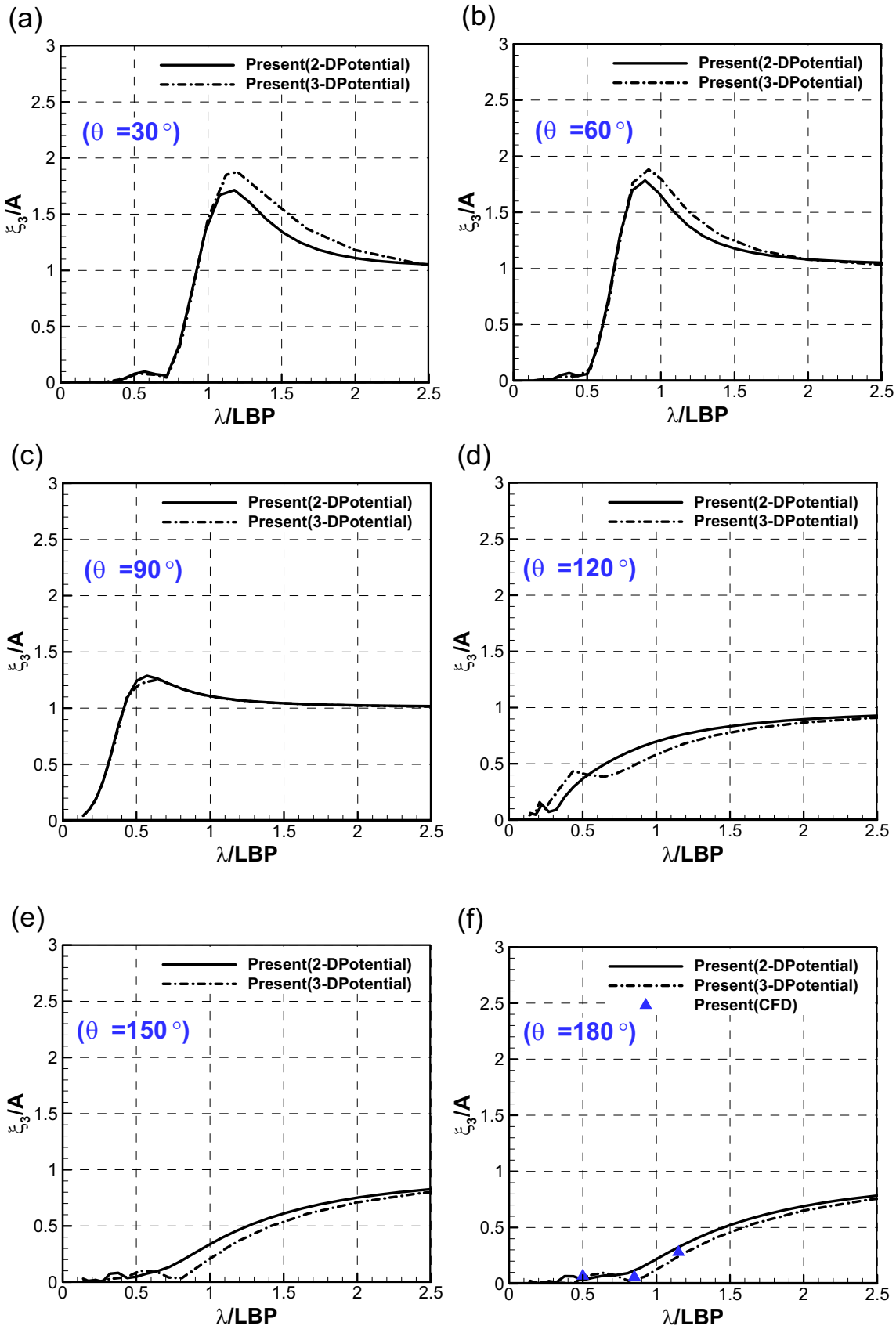


**Fig. 8.** Heave responses in various wave headings at Fn = 0.25 (θ = 30°,60°,90°,120°,150°,180°).

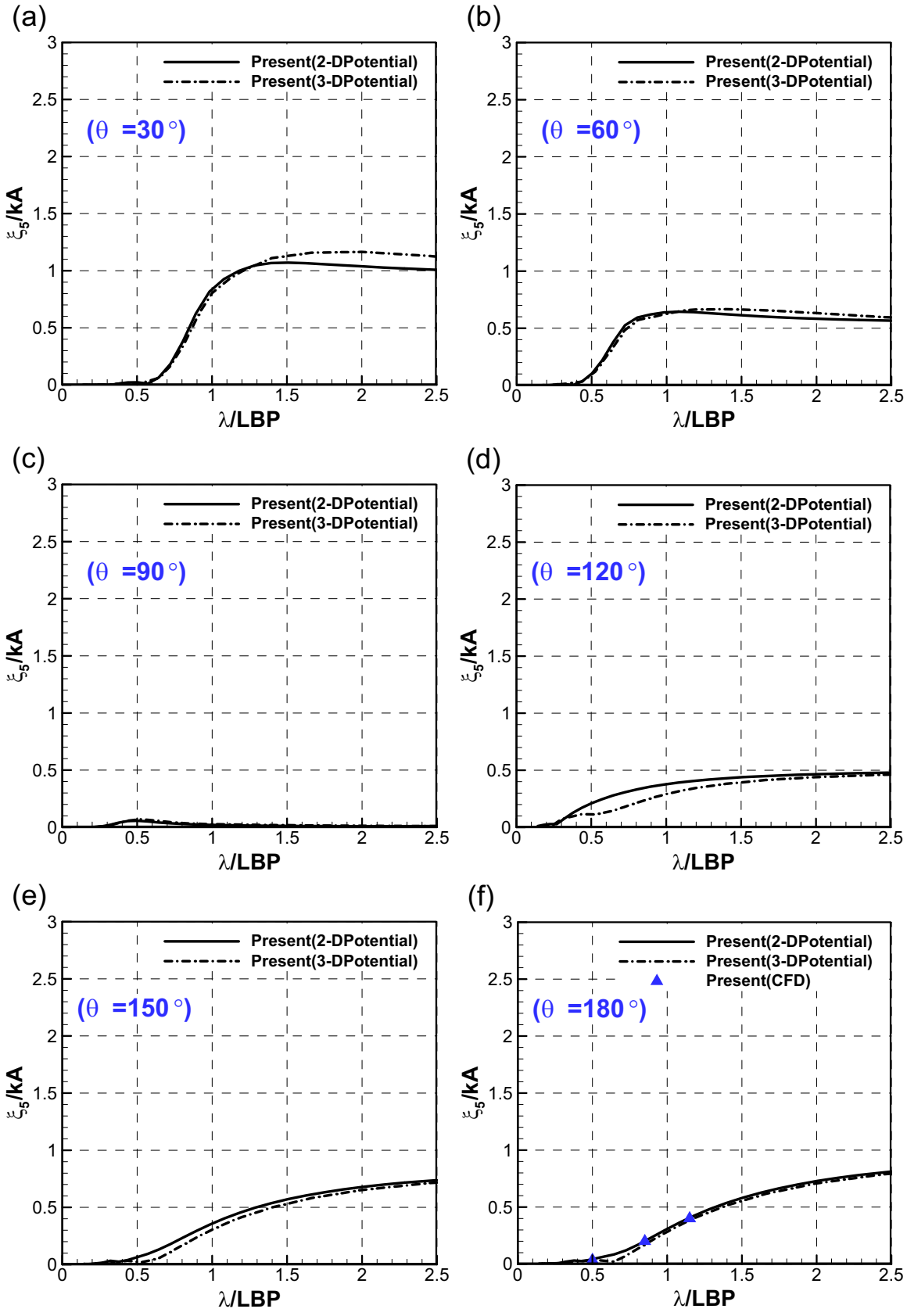


**Fig. 9.** Pitch responses in various wave headings at Fn = 0.25 (θ = 30°,60°,90°,120°,150°,180°).

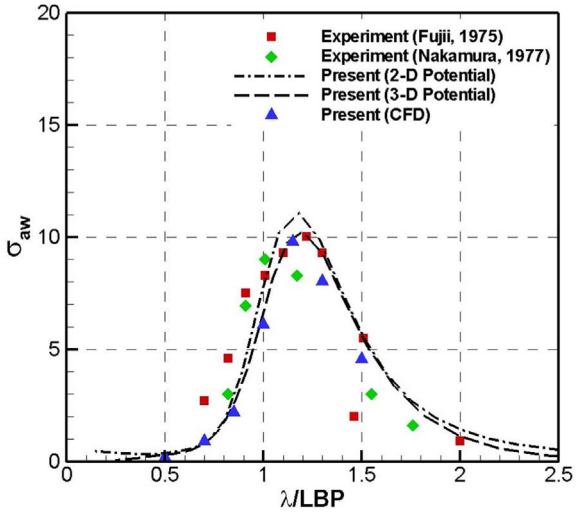


**Fig. 10.** Added resistance comparison (Fn = 0.25, θ = 0°).

### 5.1. Added resistance in regular waves

Prior to the investigation on added resistance, Response Amplitude Operators (RAOs) of heave and pitch motions are compared with the experimental data (Fonseca and Soares, 2004) in regular head waves as shown in Fig. 7. It is a well-known fact that the added resistance is proportional to the relative motions, hence heave and pitch motions, and inaccuracies in the predicted motion responses may amplify the errors in the added resistance calculations. In this study, $\xi_3$ and $\xi_5$ are the amplitudes of heave and pitch motion responses respectively whereas $k = 2\pi/\lambda$ is the wave number in deep water. The motion responses are evaluated at the ship's centre of gravity. As is illustrated in Fig. 7, the CFD method and experimental data have reasonable agreement in heave and pitch motions. The overestimation of the heave motion using the 2-D and 3-D potential methods are amplified around the resonance period ($1.0 < \lambda/L < 1.4$), while the pitch motion results obtained from both methods show good agreement with the experimental data for all wave lengths. The results of the 2-D potential flow agree reasonably well with the experimental data except around the peak value even though the heave motion is more difficult to predict accurately than the pitch motions (Bunnik et al., 2010). The 3-D potential flow over-predicts the heave motion around the heave resonance frequency and for long waves. The overestimation of the results obtained from the 3-D potential method for the heave motions can be attributed to the AFS formulation, in which the BVP is solved using zero speed Green's functions and then forward speed corrections are applied to the boundary conditions, and also to the Neumann-Kelvin (NK) approximation where the steady wave and unsteady wave interactions are linearized. Kim and Shin (2007) presented a study about the steady and unsteady flow interaction effects on advancing ships and showed that in heave and pitch responses the NK approach overestimates the heave and pitch responses compared to the experimental results, whereas the Double-Body (DB) and Steady Flow approaches agreed well with the experiments. The accuracy of the 2-D potential method is likely to stem from high encountering frequencies. As was explained previously, the 2-D potential method assumes low Froude number, high frequency and slender body approaches in the BVP solutions. Although the forward speed is high in the present problem, motion responses agree well with the experimental results because the motion responses are mainly dominated by the Froude–Krylov and restoring forces.

In addition to the vertical ship motion responses in head waves, the motions responses from the 2-D and 3-D potential methods for other wave headings are compared in Fig. 8 and Fig. 9. Similar to the heave motion in head seas, both results of 2-D and 3-D methods agree reasonably well with each other except the resonance period for the heave motion in bow waves (θ = 30° and 60°) as shown in Fig. 8(a) and (b). For following waves, the heave motion from CFD was compared additionally, which agreed reasonably with both the results of 2-D and 3-D potential methods as compared in Fig. 8(f).

Also similar to the pitch responses in head seas, both responses of 2-D and 3-D potential methods agree well with each other for other wave headings as shown in Fig. 9.

The numerical results of the added resistance using the near-field formulation are compared with the available experimental data (Fujii and Takahashi, 1975; Nakamura and Naito, 1977) as illustrated in Fig. 10, which indicates that the CFD and 2-D and 3-D potential methods both have reasonable agreement with the experimental data. In the present numerical calculation, the 3-D method estimated the added resistance slightly better than the 2-D method. This is likely to stem from the diffraction forces near the ships bow which is amplified with the increase in forward speed. Diffraction forces near the ships bow cannot be calculated accurately using the 2-D method due to the lack of properly defined bow geometry of the vessel and especially in short waves where the hydrodynamic nonlinear effects are intensified (Kashiwagi et al., 2010).

In addition to the calculation of the added resistance in head waves, validation studies on the added resistance for other wave headings are performed by comparing with experimental results by Fujii and Takahashi (1975) who carried out model tests in both regular head and oblique waves. Similarly to head seas, other wave heading directions showed similar trends using the 2-D and 3-D methods compared to the experimental data as shown in Fig. 11. For following waves, the calculation of the added resistance was performed additionally using CFD, which agreed reasonably with both the results of 2-D and 3-D potential methods and experimental data as compared in Fig. 11(f).

### 5.2. Speed loss estimation in random seas

Based on the developed approach, the speed loss due to wind and waves in random seas for the S175 containership is estimated and compared with the available simulations performed by other researchers. Among these researchers, Kwon's (2008) method is based on a semi-empirical model considering wind, vessel motions and diffraction resistance, and another study performed by Prpić-Oršić and Faltinsen (2012) estimates the ship speed loss and $CO_2$ emission which uses the ITTC spectrum in addition to considering the propeller performance in a seaway. The reference ship speed ($V_c$) in calm water is assumed to be 23 knots (Fn = 0.286) in the simulations. Fig. 12 shows the estimated ship speed loss due to waves only, and both wind and waves by the proposed approach where wind and waves are assumed to be collinear in all simulations. When only the effect of the waves are considered, the speed loss estimated in head sea by the present approach is similar to the simulated results obtained by Prpić-Oršić and Faltinsen (2012) as shown in Fig. 12. Regarding the comparison with the results predicted by Kwon's method taking into account the effect of wind and waves, the ship speed loss predicted by the present approach is lower than the simulation results based on Kwon's semi-empirical model which predicts the ship speed loss only in relation to B.N. without considering the hull form. In the present study, the developed methodology is able to estimate the ship speed loss using the resultant motions and diffraction of the hull form in the specific wave and wind parameters of speed and direction separately as well as B.N.

The achievable ship speed due to waves, and both wind and waves, with weather direction on the assumption that the directions of wind and waves are collinear is estimated at B.N. 6 as a representative sea conditions as shown in Fig. 13. If the effect of both wind and waves are considered and are assumed to be collinear, the speed loss for the wave and wind directions from head to bow seas (θ = 0–60°) is higher than the speed loss from beam directions (θ = 60–120°) and following sea

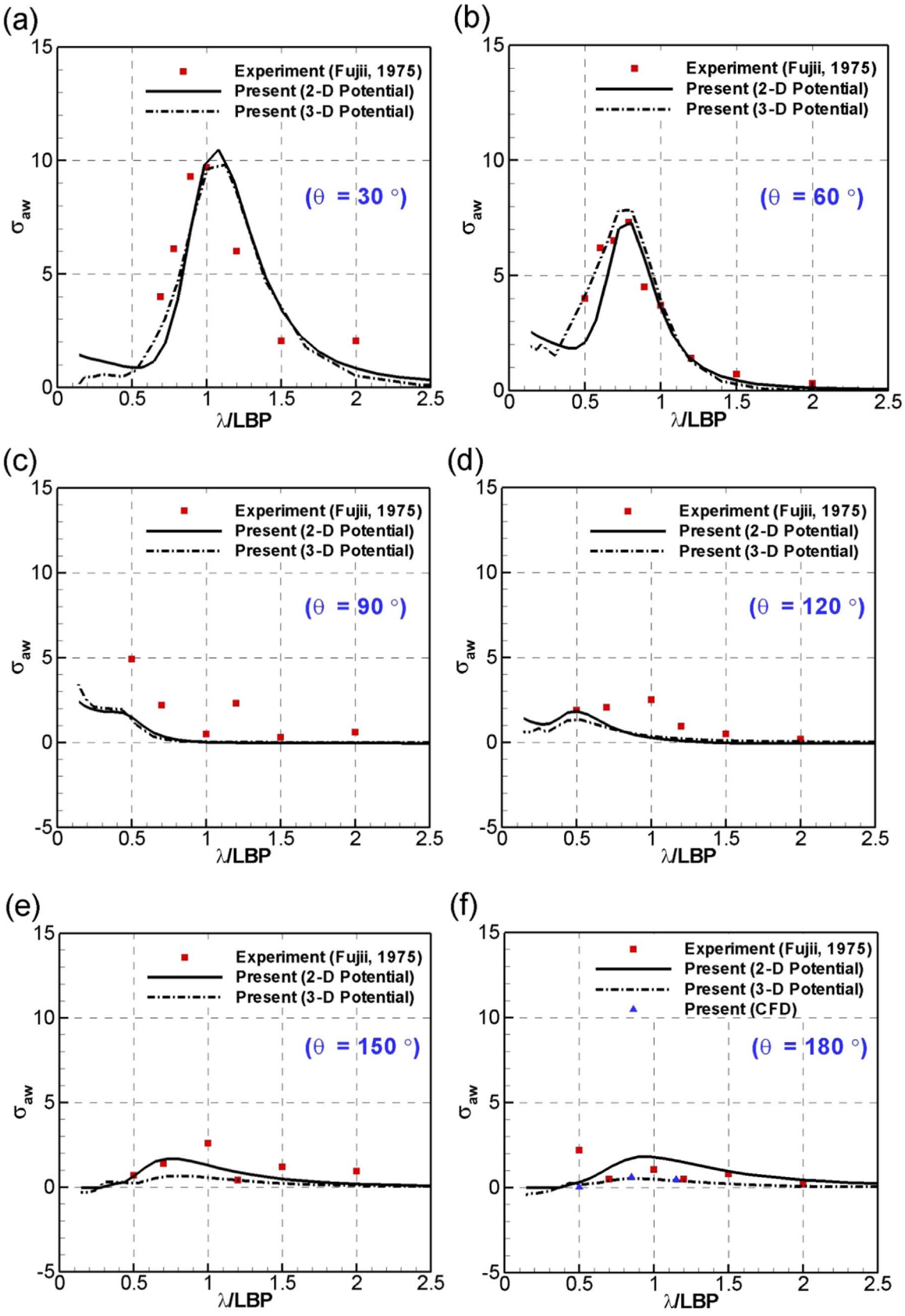


**Fig. 11.** Added resistance comparison in various wave headings at Fn = 0.25 (θ = 30°,60°,90°,120°,150°,180°).

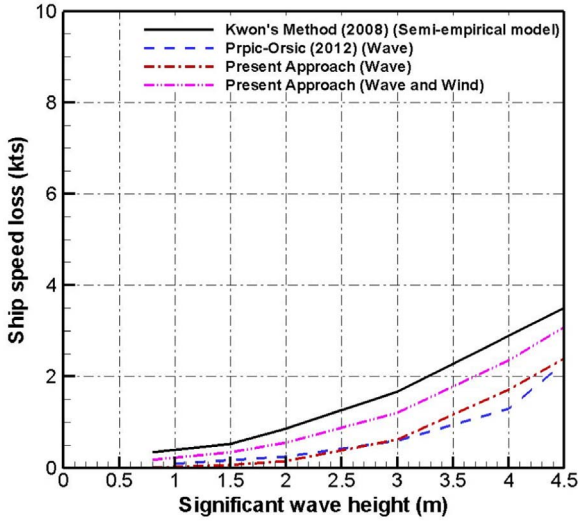


**Fig. 12.** Estimated ship speed loss due to wind and waves (Vc = 23 knots, θ = 0°).

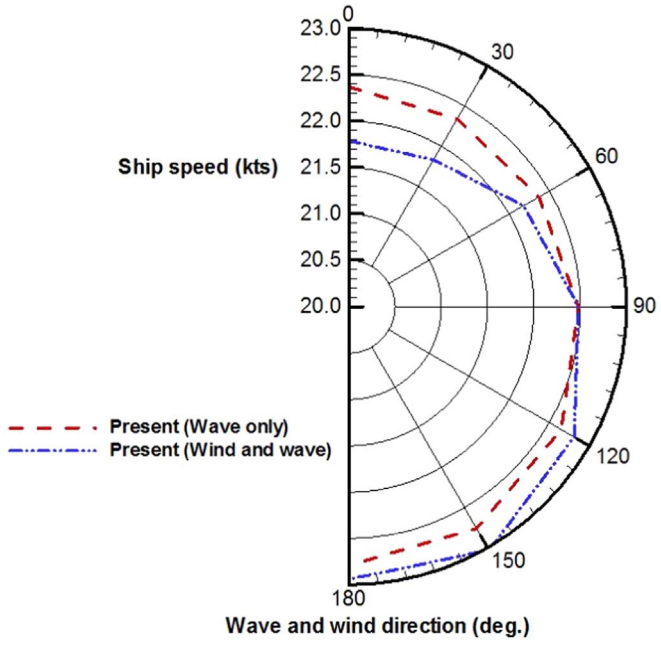


**Fig. 13.** Predicted ship speed in various weather directions (Vc = 23 knots, B.N. = 6).

**Table 5**
Predicted speed loss and sea margin with ship speed (B.N. 6, θ = 0°).

| Ship speed | 23 knots (Fn = 0.286) | 20.14 knots (Fn = 0.25) | 16.11 knots (Fn = 0.20) |
|---|---|---|---|
| Total speed loss due to wind and waves | 1.21 knots | 1.33 knots | 1.83 knots |
| Speed loss due to wind | 0.58 knots | 0.63 knots | 0.78 knots |
| Speed loss due to waves | 0.63 knots | 0.70 knots | 1.05 knots |
| Sea margin | 17.2% | 22.7% | 34.4% |

directions (θ = 120–180°). For following seas, the speed loss is less than 0.2 knots due to the wind thrusting the ship forward. From the study on the speed loss at varying directions of wind and waves, the speed loss can be estimated with the ship operating direction relative to wave and wind direction.

### 5.3. Estimation of ship speed loss and sea margin

The speed of a vessel has a dramatic impact on the fuel consumption because the speed exponentially is related to the propulsive power required. This significant potential saving makes it easy to understand why there is substantial interest in slow steaming, especially when fuel prices escalate. With consideration for the slow steaming of containership speeds, the ship speed loss at lower speeds is investigated. With the estimation of ship speed loss due to wind and irregular waves respectively, the sea margin for the ship at the representative sea condition of B.N. 6 is also investigated based on the proposed methodology for lower ship speeds ($V_c$ = 20.14 and 16.11 knots) and the assumed ship design speed ($V_c$ = 23 knots) in calm water. In this study, as summarized in Table 5, as the ship reference or operating speed is decreased, the ship speed loss increases and higher sea margin is needed to achieve the same reference ship speed at the sea conditions at B.N. 6. The differences in the ship speed reduction due to wind and waves based on the change in the reference speed from 23 knots to 16.11 knots are 0.2 knots and 0.42 knots respectively, thus when the ship reference speed decreases, the effect of the ship speed loss due to waves is higher than that for wind. Furthermore, when the ship speed is decreased, the corresponding sea margin is increased, whereas the absolute value of the required additional power is decreased.

## 6. Conclusions

A reliable methodology to estimate the added resistance and ship speed loss of the S175 containership due to wind and waves in a seaway was proposed using the Pierson-Moskowitz spectrum, depending on the significant wave height and mean wave period parameters corresponding to each B.N. up to 7. The reduction in ship speed was estimated using the developed approach and was compared with simulation results predicted by other researchers. Based on comparison results of the ship speed loss due to wind and waves and considering actual sea conditions for ship operation, the capability of the developed approach to predict the ship speed loss in realistic sea conditions was investigated in detail. From the estimated results of the ship speed loss due to wind and waves, at low B.N., the effect of wind on the ship speed loss was observed to be higher than that of waves, however at higher B.N., which means that the sea condition was getting more severe, the speed loss due to waves was larger than that due to wind. At the representative sea conditions of B.N. 6, the speed losses due to only wind, and both wind and waves, were predicted with respect to weather direction. From the study on the speed loss at varied directions of wind and waves, the speed loss can be estimated with the ship operating direction relative to weather direction. In head seas especially, the total speed loss was estimated to be 1.21 knots (0.58 knots due to wind and 0.63 knots due to waves) whilst the required sea margin was predicted to be 17.2%.

The proposed methodology was developed considering the latest IMO and ITTC guidelines/recommendations. Therefore, this study will be helpful for the calculation of fw in the EEDI formulation and the hence assessment of the environmental impact of ship emissions. Also, with the ship main particulars and hull form lines, even in the ship design stage once the general hull form is set, it is possible to optimize the hull form for better performance not only in calm water but also in a seaway considering the speed loss and ship motions, which are related to ship safety and efficiency in operation. In the developed approach, the prediction methods for the added resistance can be updated (e.g. wind tunnel test results of the ship instead of using the Blendermann chart as general empirical chart for the prediction of the added resistance due to wind).

Before predicting the added resistance and ship speed loss due to wind and irregular waves, a wide range of validation studies was performed for the added resistance with ship motions in regular head and oblique seas using the 2-D and 3-D linear potential theories and

unsteady RANS simulations by CFD.

From validation studies for the motions of heave and pitch and the added resistance compared with the available experimental data, the characteristics of the 2-D and 3-D linear potential methods and CFD were investigated and the numerical results were found to agree reasonably well with the experimental data in regular head and oblique seas. For following seas, the calculation of the added resistance was additionally performed using CFD, which also showed reasonable agreement with the 2-D and 3-D potential method results and experimental data.

Reduction in ship speed and the required sea margin due to wind and waves to achieve the initial reference speed ($V_c$) were investigated at B.N. 6, which was adopted by the MEPC as the representative sea conditions for two lower speeds ($V_c$ = 20.14 and 16.11 knots) and the assumed ship design speed ($V_c$ = 23 knots) in head wave and wind conditions. This study indicates that as the ship reference or operating speed is decreased, total speed loss due to both wind and waves increases, especially due to waves. It should be noted that if a ship operator would order a reduction in ship speed, the difference between the specified speed and the actual ship speed increases for the same wind and wave conditions in a seaway. Also, the estimated sea margin is significantly increased when the initial reference speed is decreased, even though the absolute value of the required additional power is reduced. At the ship reference speed of 16.11 knots, almost 35% of sea margin would be required to maintain operation at the same speed.

For future work, further study on the prediction of the added resistance with ship motions for other ship types, especially blunt hulls such as crude oil tankers and bulkers, and further development of a reliable methodology to estimate the ship speed loss using 2-D as well as 3-D potential methods in head and oblique sea conditions including other effects such as ship draught and the change in propulsive performance will be carried out. Finally, it would be interesting to develop the forebody hull of a vessel to reduce the ship speed loss in a seaway considering actual operating conditions.

## Acknowledgements

The authors are grateful to the Engineering and Physical Research Council (EPSRC) for funding the research reported in this paper through the project: “Shipping in Changing Climates” (EPSRC grant no. EP/K039253/1).

The results given in the paper were obtained using the EPSRC funded ARCHIE-WeSt High Performance Computer (www.archie-west.ac.uk). EPSRC grant no. EP/K000586/1.

## References

Arribas, F., 2007. Some methods to obtain the added resistance of a ship advancing in waves. Ocean Eng. 34 (7), 946–955.

Banks, C., Turan, O., Incecik, A., Theotokatos, G., Izkan, S., Shewell, C., Tian, X., 2013. Understanding ship operating profiles with an aim to improve energy efficient ship operations. In: Proceedings of the Low Carbon Shipping Conference. London, UK, pp. 9–10.

Blendermann, W., 1994. Parameter identification of wind loads on ships. J. Wind Eng. Ind. Aerodyn. 51 (3), 339–351.

Boese, P., 1970. Eine einfache Methode zur Berechnung der Widerstandserhöhung eines Schiffes im Seegang. Schr. Schiffbau 17, 86.

Bunnik, T., van Daalen, E., Kapsenberg, G., Shin, Y., Huijsmans, R., Deng, G., Delhommeau, G., Kashiwagi, M., Beck, B., 2010. A comparative study on state-of-the-art prediction tools for seakeeping. In: Proceedings of the 28th Symposium on Naval Hydrodynamics. Pasadena, CA.

Deng, G., Leroyer, A., Guilmineau, E., Queutey, P., Visonneau, M., Wackers, J., 2010. Verification and validation for unsteady computation. In: Proceedings of Gothenburg 2010: A Workshop on CFD in Ship Hydrodynamics, Gothenburg, Sweden.

Faltinsen, O.M., Minsaas, K.J., Liapis, N., Skjørdal, S.O., 1980. Prediction of resistance and propulsion and propulsion of a ship in a seaway. In: Proceedings of the 13th Symposium on Naval Hydrodynamics. Tokyo, pp. 505–529.

Fonseca, N., Soares, C.G., 2004. Experimental investigation of the nonlinear effects on the vertical motions and loads of a containership in regular waves. J. Ship Res. 48 (2), 118–147.

Fujii, H., Takahashi, T., 1975. Experimental study on the resistance increase of a ship in regular oblique waves. In: Proceedings of the 14th ITTC. 4, pp. 351–360.

Gerritsma, J., Beukelman, W., 1972. Analysis of the resistance increase in waves of a fast cargo ship. Int. Shipbuild. Prog. 19 (217).

Gothenburgh, 2010. A Workshop on Numerical Ship Hydrodynamics. Denmark.

Guo, B., Steen, S., Deng, G., 2012. Seakeeping prediction of KVLCC2 in head waves with RANS. Appl. Ocean Res. 35, 56–67.

Havelock, T.H., 1937. The resistance of a ship among waves. Proc. R. Soc. Lond. Ser. A Math. Phys. Sci., 299–308.

Hizir, O.G., 2015. Three Dimensional Time Domain Simulation of Ship Motions and Loads in Large Amplitude Waves. Naval Architecture, Ocean and Marine Engineering, University of Strathclyde, Glasgow.

Holtrop, J., 1984. A statistical re-analysis of resistance and propulsion data. Int. Shipbuild. Prog. 31 (363), 272–276.

Holtrop, J., Mennen, G., 1978. A statistical power prediction method. Int. Shipbuild. Prog. 25, 290.

Holtrop, J., Mennen, G., 1982. An Approximate Power Prediction Method.

IMO, 2009. Guidelines for Voluntary Use of the Ship Energy Efficiency Operational Indicator (EEOI). International Maritime Organisation (IMO), London.

IMO, 2011. Amendments to the Annex of the Protocol of 1997 to Amend the International Convention for the Prevention of Pollution From Ships, 1973, as Modified by the Protocol of 1978 Relating Thereto. International Maritime Organisation (IMO), London.

IMO, 2012. Interim Guidelines for the Calculation of the Coefficient $f_w$ for Decrease in Ship Speed in a Representative Sea Condition for Trial Use. International Maritime Organisation (IMO), London.

ITTC, 2014. The Seakeeping Committee. Technical Report, Copenhagen, Denmark.

Joncquez, S.A., 2009. Second-Order Forces and Moments Acting on Ships in Waves (Ph.D. thesis). Technical University of Denmark, Copenhagen, Denmark.

Joosen, W.P.A., 1966. Added resistance of ships in waves. In: Proceedings of the 6th Symp. on Naval Hydrodynamics. National Academy Press, Washington D.C.,USA.

Kashiwagi, M., Ikeda, T., Sasakawa, T., 2010. Effects of forward speed of a ship on added resistance in waves. Int. J. Offshore Polar Eng. 20 (03).

Kim, B., Shin, Y.S., 2007. Steady flow approximations in three-dimensional ship motion calculation. J. Ship Res. 51 (3), 229–249.

Kim, H.T., Kim, J.J., Choi, N.Y., Lee, G.H., 2014. A study on the operating trim, shallow water and wave effect. SNAK, 631–637.

Kim, K.H., Kim, Y., Kim, Y., 2007. WISH JIP Project Report and Manual. Marine Hydrodynamic Laboratory, Seoul National University.

Kim, K.H., Seo, M.G., Kim, Y.H., 2012. Numerical analysis on added resistance of ships. Int. J. Offshore Polar Eng. 22 (01), 21–29.

Kwon, Y.J., 2008. Speed loss due to added resistance in wind and waves. Nav. Archit., 14–16.

Lee, C.H., Sclavounos, P.D., 1989. Removing the irregular frequencies from integral equations in wave-body interactions. J. Fluid Mech. 207, 393–418.

Liu, S., Papanikolaou, A., Zaraphonitis, G., 2011. Prediction of added resistance of ships in waves. Ocean Eng. 38 (4), 641–650.

Loukakis, T., Sclavounos, P., 1978. Some extensions of the classical approach to strip theory of ship motions, including the calculation of mean added forces and moments. J. Ship Res. 22, 1.

Mauro, H., 1960. The drift of a body floating on waves. J. Ship Res. 4, 1–5.

McTaggart, K., Datta, I., Stirling, A., Gibson, S., Glen, I., 1997. Motions and Loads of a Hydroelastic Frigate Model in Severe Seas. DTIC Document.

Moctar, B., Kaufmann, J., Ley, J., Oberhagemann, J., Shigunov, V., Zorn, T., 2010. Prediction of ship resistance and ship motions using RANSE. In: Proceedings of the Workshop on Numer. Ship Hydrodyn. Gothenburg, p. l.

Nakamura, S., Naito, S., 1977. Propulsive performance of a container ship in waves. Nav. Archit. Ocean Eng. 15, 24–48.

Newman, J.N., 1967. The drift force and moment on ships in waves. J. Ship Res. 11 (1), 51–60.

Park, D.M., Seo, M.G., Lee, J., Yang, K.Y., Kim, Y., 2014. Systematic experimental and numerical analyses on added resistance in waves. J. Soc. Nav. Archit. Korea 51 (6), 459–479.

Prpić-Oršić, J., Faltinsen, O.M., 2012. Estimation of ship speed loss and associated CO 2 emissions in a seaway. Ocean Eng. 44, 1–10.

Sadat-Hosseini, H., Carrica, P., Kim, H., Toda, Y., Stern, F., 2010. URANS simulation and valiation of added resistance and motions of the KVLCC2 crude carrier with fixed and free surge conditions. In: Proceedings of Gothenburg 2010: A Workshop on CFD in Ship Hydrodynamics.

Sadat-Hosseini, H., Wu, P., Carrica, P., Kim, H., Toda, Y., Stern, F., 2013. CFD verification and validation of added resistance and motions of KVLCC2 with fixed and free surge in short and long head waves. Ocean Eng. 59, 240–273.

Salvesen, N., Tuck, E.O., Faltinsen, O.M., 1970. Ship Motions and Sea Loads SNAME. 104, pp. 119–137.

SHOPERA, 2016. Energy Efficient Safe Ship Operation EU FP-7 Project.

SIMMAN, 2014. Workshop on Verification and Validation of Ship Manoeuvring Simulation Methods. Denmark.

Simonsen, C.D., Otzen, J.F., Joncquez, S., Stern, F., 2013. EFD and CFD for KCS heaving and pitching in regular head waves. J. Mar. Sci. Technol. 18 (4), 435–459.

Stern, F., Xing, T., Yarbrough, D.B., Rothmayer, A., 2006. Hands-on CFD educational interface for engineering courses and laboratories. J. Eng. Educ. 95 (1), 63.

Tezdogan, T., Demirel, Y.K., Kellett, P., Khorasanchi, M., Incecik, A., Turan, O., 2015. Full-scale unsteady RANS CFD simulations of ship behaviour and performance in head seas due to slow steaming. Ocean Eng. 97, 186–206.

Van't Veer, A.P., 2009. PRECALv6.5 Theory Manual.

Wright, J., Colling, A., Park, D., 1999. Waves, Tides, and Shallow-Water Processes. Gulf Professional Publishing.